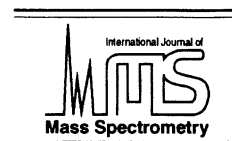




ELSEVIER

International Journal of Mass Spectrometry 213 (2002) 63–80



www.elsevier.com/locate/ijms

High temperature chemistry of molten glass ion emitters

G.F. Kessinger, J.E. Delmore*

Idaho National Engineering and Environmental Laboratory, Idaho Falls, Idaho 83415, USA

Received 23 April 2001; accepted 8 August 2001

Abstract

Thermodynamic calculations have been performed to predict the chemical behavior of ten elements in molten borosilicate glass to gain new insights into the ion formation mechanisms for this class of ion emitters. General trends identified during the computational studies include: (1) all of the analyte elements studied are reduced, at least in part, to the elemental state (which is predicted to be soluble in the molten glass); (2) a finite percentage of each of the analytes volatilizes in the elemental state, with a possibility that an electron will be stripped to form a positive ion; (3) dilution of the element in the molten glass matrix tends to reduce the evaporation rate of the analyte element for a given temperature (as compared to the pure material), allowing vaporization to occur evenly and at higher temperatures; and (4) rhenium, dissolved from the supporting filament, is predicted to be present in the molten glass. This Re is probably present as an oxide, which is believed to enhance ion emission probabilities by increasing the work function of the surface. The results of this study support the hypothesis that the ion formation mechanism for the elements investigated involves the volatilization of the element as both neutral and ionic atomic species, possibly as a Saha-Langmuir type process. Other ion emission processes are probably active for those analytes that are not easily reduced to the elemental state in the molten glass matrix. (Int J Mass Spectrom 213 (2002) 63–80) © 2002 Elsevier Science B.V.

Keywords: Thermal ionization; Silica gel; Molten glass; Isotope ratios; Ion emission mechanisms

1. Introduction

The thermal ion formation process generally termed the “silica gel” method has been widely used for producing ions for isotope ratio measurements by thermal ionization mass spectrometry (TIMS) since its introduction in 1969 [1]. The original study concentrated on the analysis of lead (Pb), and has been extended for the analysis of other elements, including the ten elements addressed in this study (see Table 1). In the original method, the emitter was produced by

evaporating to dryness a mixture of phosphoric acid, an aqueous solution containing the element to be analyzed, and hydrated silica gel that had been applied to a rhenium filament. Subsequent heating of the filament melts the mixture into a glass and results in the emission of thermal ions. Other investigators discovered that boric acid worked as well as, and in some cases better than, phosphoric acid [2] to produce the glass emitters, although the majority of analyses are still conducted using phosphoric acid. The fundamental mechanisms by which these processes produce ions is only partially understood, although in earlier publications [3,4] at least a few of the features were identified. The present study was undertaken in an

* Corresponding author. E-mail: jed2@inel.gov

Table 1
Metals analyzed by silica-gel TIMS method

Analyte	Species	“Enhancer” components	Support	T (K)	Reference
Ag	Ag ⁺	Silica gel, H ₃ PO ₄	Re	1273	[47]
Ag	Ag ⁺	Silica gel, H ₃ PO ₄	Re	Not measured	[44]
Ag	Ag ⁺	Silica gel, H ₃ PO ₄	Re	1273	[48]
Cd	Cd ⁺	Silica gel, H ₃ PO ₄	Re	Not measured	[52]
Cd	Cd ⁺	Silica gel, H ₃ PO ₄	Re	Not measured	[44]
Cd	Cd ⁺	Silica gel, H ₃ PO ₄	not reported	1523–1673	[51]
Cd	Cd ⁺	Silica gel, H ₃ PO ₄	Re	1373–1573	[41]
Cr	Cr ⁺	SiO ₂ , GeO _x	W	1523	[53]
Cr	Cr ⁺	SiO ₂ , B ₂ O ₃	W	1423–1463	[54]
Fe	Fe ⁺	Silica gel, B ₂ O ₃	Re	1593–1613	[2]
Fe	Fe ⁺	Silica gel, B ₂ O ₃	Re, Pt	1423	[56]
Fe	Fe ⁺	SiO ₂ , B ₂ O ₃	Pt	1473	[55]
Ni	Ni ⁺	SiO ₂ , GeO _x	W	Not reported	[57]
Ni	Ni ⁺	SiO ₂ , GeO _x	W	1523	[53]
Pb	Pb ⁺	Silica gel, H ₃ PO ₄	Re	Not measured	[44]
Pb	Pb ⁺	Silica gel	Re	1523	[43]
Pb	Pb ⁺	Silica gel, H ₃ PO ₄	Re	1373–1573	[1]
Pb	Pb ⁺	Silica gel, H ₃ PO ₄	Re	1473–1673, 1773	[42]
Pb	Pb ⁺	Silica gel, H ₃ PO ₄	Re	1373–1573	[41]
Pb	Pb ⁺	Silica gel, H ₃ PO ₄	Re	1473	[46]
Te	Te ⁺	Silica gel, H ₃ PO ₄	Re	1523–1573	[47]
Te	Te ⁺	Silica gel, H ₃ PO ₄	Re	Not measured	[58]
Tl	Tl ⁺	Silica gel, H ₃ PO ₄	Re	973	[59]
Tl	Tl ⁺	Silica gel, H ₃ PO ₄	Re	973	[41]

effort to expand the understanding of the chemistry of these ion emitters.

A model was presented in a previous publication [4] in which it was shown both experimentally and computationally, that Ag in Ag-containing molten glasses is present in the zero oxidation state in the condensed phase and that the atoms volatilize as both neutral and ionic atomic species. This was demonstrated by measuring the thermal desorption profiles for Ag ions and neutrals from Ag-containing borosilicate glasses, and showing that the thermal desorption profiles have substantial overlap, providing supporting evidence that neutrals and ions originate from the same Ag species, namely the elemental state. Originally, it seemed counter intuitive that a metal oxide would be reduced while dissolved in an oxide matrix but both the experimental and computational results support this concept. It is believed that the ratio of ionic to neutral species volatilizing from the surface is determined largely by the work function of the surface

and the ionization potential of the evaporating atom. The difficulty with this hypothesis is that the ionization potentials for these elements are 2–4 eV higher than the work functions measured for some common mixed oxide systems containing Si, which tend to be about 5 eV or less [5]. For this hypothesis to be believable, the work function of the glass needs to be much higher than 5 eV. A model for how such a high work function may be possible was offered [4], based upon computational and limited experimental evidence. That work has been extended in the present study, which includes thermodynamic computations that support the extension of this model to nine other elements.

Other investigators have conducted electrochemical studies on molten glasses in order to determine the oxidation states of various solute elements [6–34], although the chemical makeup of these glasses were substantially different from those used in the silica gel method. In addition, the electrochemical studies were

performed under an oxidizing atmosphere (air), whereas the silica gel method involves volatilization under a high vacuum, which is a reducing atmosphere (as compared to air). It is suspected that the analyte elements in the electrochemistry experiments will be shifted toward a higher oxidation state because of the presence of atmospheric air. While the electrochemistry studies are still believed to be relevant, this possible shift in oxidation states needs to be considered when comparing the two types of experiments.

2. Computational studies

Two types of calculations were performed: evaporation rate calculations and thermochemical modeling calculations. The evaporation rate calculations were performed to predict the temperature required to evaporate approximately 50% of the analyte element during a 40 min analysis. The purpose of the thermochemical modeling calculations was to predict the equilibrium state of the materials during analyses. These calculations predict only what is thermodynamically possible; kinetic factors are not addressed and it is likely that thermodynamic equilibrium might never be reached under the actual experimental conditions. These molten glasses are extremely viscous, [3] particularly at lower temperatures, and the time involved for analyte elements to migrate to the surface could be considerable. The kinetic factor relating to reduced migration rates in the viscous medium is the probable reason why the actual volatilization rates are well below those predicted by thermodynamic calculations for the more volatile elements. Another significant circumstance is that the calculations presented here are for molten borosilicate glasses, while the majority of experimental work has been conducted with phosphosilicate glasses. This fact may explain some of the differences between the calculated and experimental temperatures. Boric acid, rather than phosphoric acid, was used in the calculations because the thermodynamic data set for the B–O system is more complete.

2.1. Evaporation rate calculations and results

One of the mechanisms hypothesized to explain how molten glass matrices enhance ion emission is that the analyte element is dissolved and solvated in the molten borosilicate glass, reducing the analyte vapor pressure (as compared to its vapor pressure in its pure state). This allows the vaporization, which normally takes 30–60 min, to occur at higher temperatures where the ratio of ions to neutrals would be expected to be greater (based on the Saha-Langmuir theory). Calculations of evaporation rates were performed to test this hypothesis, and to determine the “ideal” evaporation rate of the analyte from the molten glass solution. Because silica gel analyses are commonly 30–60 min in duration, with approximately 50% of the analyte exhausted during the analysis, calculations were performed to identify the temperatures at which the analyte element would be exhausted to about 50% of the initial mass. It was assumed that the evaporation rate of the analyte in the silica gel matrix was equal to the sum of the rates for all of the significant analyte-bearing species (monomer, dimer, oxide, etc). Vapor pressures for the analyte of interest, in the molten glass matrix, were computed using the FACT EQUILIB code [35], the use of which was described in an earlier publication [4].

The speciation, temperature and vapor pressure results from the thermochemical equilibrium calculations were used as input for the computation of the evaporation rate. It was assumed that 9.27 nmol of analyte were present in the silica gel mixture as an oxide (nitrate in the case of Ag), that the molar mass of the vaporizing species was the weighted average of the most important metal-bearing vapor species, and that the time interval was 40 min. The Hertz-Knudsen-Langmuir equation (HKL), which describes the functional relationships of the vapor pressure, temperature, evaporation surface area, molar mass of the evaporating species, and rate of evaporation to one another, was used to compute the evaporation rate results. It may be integrated and written as

$$n = p_o at / (2\pi MRT)^{1/2}$$

Table 2

Vapor pressures and temperatures at which approximately 50% of the metal in a metal oxide-silica-gel sample would be depleted in 40 min^a

Metal oxide	Experimental temperature (k)	Calculation temperature ^b (k)	ΔT^c (k)	Calculated pressure ^d (atm)
PbO ₂ ^e	1573	1048	525	1.72×10^{-9}
AgNO ₃ ^e	1273	973	300	2.80×10^{-9}
CdO ^e	1573	598	975	2.14×10^{-9}
Cr ₂ O ₃	1473	1648	-175	2.70×10^{-9}
FeO	1593	1473	120	1.67×10^{-9}
NiO ^e	1523	1473	50	2.07×10^{-9}
Te ₂ O ₃ ^e	1558	583	975	3.97×10^{-9}
TiO ₂ ^e	973	723	250	3.80×10^{-9}
Bi ₂ O ₃	1273	823	450	1.11×10^{-9}
Au ₂ O ₃	None reported	1373	Not applicable	2.72×10^{-9}

^aFor these calculations, a silica-gel surface 0.03×0.03 in was assumed.

^bTemperatures rounded to 5 degree intervals.

^c ΔT = experimental temperature from column 2 – calculation temperature from column 3.

^dTotal pressure of all metal-bearing species.

^eExperimental work performed with phosphorosilicate glass.

where n is the number of moles evaporated, p_o is the observed vapor pressure, a is the surface area from which evaporation is occurring, t is the time over which the evaporation occurs, M is the molar mass of the vapor species (or weighted mean molar mass for mixtures of species), R is the ideal gas constant, and T is the absolute temperature. If the vaporization coefficient, $\alpha = p_o/p_{eq}$, which can have values $0 \leq \alpha \leq 1$, is unity, then p_o is equivalent to the equilibrium vapor pressure, p_{eq} ; if not, then the equilibrium vapor pressure is greater than the observed pressure.

Because the input to the HKL equation was a pair of values, temperature and pressure (T - P pair), the calculations were performed in an iterative fashion, until an “ n ” corresponding to about 50% of the initial amount of analyte was generated. These T - P pairs are presented in Table 2, along with averages of the experimental temperatures from Table 1 and the temperature differences between the calculated and average experimental temperatures. The computed vapor pressures were also compared to the vapor pressures (computed using the FACT EQUILIB code [35] as described in Sec. 2.2) of the analyte of interest over the pure material. In all situations a higher temperature was required to produce a given vapor pressure of the element from the molten glass than from the pure

material. The differences between the temperatures computed for the pure materials and the materials in molten glass are presented in Table 3.

As can be seen in Table 2, the experimental temperature is higher than the calculated temperature for all cases except Cr. Worth noting is that the three elements with the smallest temperature differential, Cr, Ni, and Fe, are analyzed at the highest temperature. It appears that a threshold temperature must be reached to reduce the viscosity of the melt enough so the evaporation rate is not diffusion limited. The implications of these results are that kinetic factors play an important role and that systems where the analytes volatilize at lower temperatures are far from thermodynamic equilibrium, corresponding to a more viscous molten glass. This situation limits the extent to which thermodynamics can be used to quantify the chemistry of these systems, particularly those with solutes that are volatile at the lower temperatures, although the thermodynamic results may still be useful for a more qualitative understanding. Based upon these observations, it is assumed that the lower the temperature the farther the systems are from equilibrium (due to the viscosity of the glass). Many of the calculations predict that the glass is highly depleted at the end of the analysis, particularly of the

Table 3

Vapor pressures of pure metals at temperature T and metal pressures over oxides dissolved in silica-gel solutions at 1173 K

Metal	T (K) ^a	(1173 – T)(K)	Vapor pressure over metal at temperature T (atm)	Vapor pressure over silica-gel solution at 1173 K (atm)
Pb	748	425	8.69×10^{-9}	8.71×10^{-9}
Ag	1008	165	8.48×10^{-9}	8.35×10^{-9}
Cd	410	763	9.13×10^{-9}	9.27×10^{-9}
Cr	824	350	1.98×10^{-18}	2.01×10^{-19}
Fe ^b	1004	169	2.55×10^{-14}	2.59×10^{-14}
Fe ^c	984	189	9.62×10^{-15}	9.61×10^{-15}
Ni	1118	55	4.78×10^{-13}	4.84×10^{-13}
Te	745	428	8.74×10^{-9}	8.93×10^{-9}
Tl	676	497	9.38×10^{-9}	9.27×10^{-9}
Bi	764	409	9.10×10^{-9}	9.27×10^{-9}
Au	1103	70	2.20×10^{-11}	2.17×10^{-11}

^aTemperature rounded to nearest degree.^bCompared to FeO in silica-gel.^cCompared to Fe₂O₃ in silica-gel.

boron oxide component, yet the molten glass is still largely intact at the end of an actual analysis. This observation is consistent with evaporation coefficients less than unity.

2.2. Thermodynamic modeling calculations

Each of the ten analytes considered in this study has been analyzed by the silica gel method; published information about these systems is presented in Table 1. For the present work, only the silica gel-B₂O₃ system was considered. The elements were each considered as the oxide because data for nitrates other than AgNO₃ were unavailable. Some of the referenced studies used matrices other than borosilicate, and these are noted in Table 1. This could skew the results where the analysis temperature is for a phosphosilicate matrix and the calculated temperature is for a borosilicate temperature; asterisks in Table 2 indicate these cases.

Additional calculations were performed to examine the chemical equilibria (solid–liquid–vapor equilibria) of each analyte in the elemental state, the chemical equilibria (solid–liquid–vapor equilibria) of each analyte element as either a pure oxide or nitrate, and the chemical equilibria (solid–liquid–vapor equilibria) of chemical systems containing borosilicate

glass and the Re filament. The calculations on the elemental states (Table 3), and the pure oxides and nitrate (Table 4), were performed to provide baseline vapor pressures against which the vapor pressures of the analytes and their oxides computed for the silica gel systems could be compared. The calculations on the silica gel-refractory metal systems (Table 5) were performed to compare the computed solubilities of these refractory metals to the Re solubilities computed during the analyte-silica gel calculations.

In earlier work [4], calculations were performed on chemical systems that included other filament materials; however, the only filament material reported here is Re, primarily because the bulk of the experimental work reported in the literature has been performed with Re filaments. The earlier calculations demonstrated two major reasons why Re makes a good filament material for these applications. First, Re does not significantly reduce the glass components (B₂O₃ and SiO₂) even though the thermodynamic calculations indicate that it can reduce a number of oxides and nitrates of analytes. Second, when Re oxidizes it does not form an insoluble, crystalline phase that mixes with the molten glass, which appears to be a significant problem with Ta filaments. Instead, the Re oxides that do form are volatile and are hypothesized to migrate to the surface of the molten

Table 4
Predicted Speciation/Phase Behavior of Pure Metal Oxides at High Temperatures

Initial phase	Temp (K)	Crystalline phases	Liquid speciation	Mole fraction	Vapor speciation	Pressure (atm) ^a
PbO ₂ ^b	1573	None	None		Pb O ₂ O PbO	8.71 × 10 ⁻⁹ 8.51 × 10 ⁻⁹ 9.57 × 10 ⁻¹⁰ 5.64 × 10 ⁻¹⁰
AgNO ₃	1273	Ag	None		O ₂ N ₂ Ag NO O Ag ₂ NO ₂	1.77 × 10 ⁻³ 5.88 × 10 ⁻⁴ 8.22 × 10 ⁻⁸ 9.10 × 10 ⁻⁷ 4.49 × 10 ⁻⁹ 3.34 × 10 ⁻⁹ 9.81 × 10 ⁻¹⁰
CdO ^b	1573	None	None		Cd O ₂ O	9.27 × 10 ⁻⁹ 4.29 × 10 ⁻⁹ 6.80 × 10 ⁻¹⁰
Cr ₂ O ₃	1473	Cr ₂ O ₃	None		Cr O CrO	5.64 × 10 ⁻¹² 4.31 × 10 ⁻¹² 3.03 × 10 ⁻¹²
FeO ^b	1593	None	None		Fe O ₂ O FeO	8.67 × 10 ⁻⁹ 6.13 × 10 ⁻⁹ 1.04 × 10 ⁻⁹ 6.04 × 10 ⁻¹⁰
Fe ₂ O ₃ ^b	1593	None	None		Fe O ₂ O FeO	8.78 × 10 ⁻⁹ 6.13 × 10 ⁻⁹ 1.04 × 10 ⁻⁹ 6.04 × 10 ⁻¹⁰
NiO ^b	1523	None	None		Ni O ₂ O	9.23 × 10 ⁻⁹ 4.43 × 10 ⁻⁹ 3.65 × 10 ⁻¹⁰
TeO ₂ ^b	1558	None	None		Te O ₂ O TeO	9.16 × 10 ⁻⁹ 8.81 × 10 ⁻⁹ 8.08 × 10 ⁻¹⁰ 1.09 × 10 ⁻¹⁰
Tl ₂ O ₃ ^b	973	None	None		Tl O ₂	9.27 × 10 ⁻⁹ 6.95 × 10 ⁻⁹
Bi ₂ O ₃	1273	None	Bi ₂ O ₃ Bi	0.980 2.07 × 10 ⁻²	O ₂ Bi BiO Bi ₂ O	4.35 × 10 ⁻⁵ 3.95 × 10 ⁻⁵ 1.28 × 10 ⁻⁵ 1.20 × 10 ⁻⁴ 7.05 × 10 ⁻¹⁰
Au ₂ O ₃	1273	Au	None		O ₂ O Au	8.84 × 10 ⁻⁴ 4.30 × 10 ⁻⁹ 3.18 × 10 ⁻⁹

^aValues less than 10⁻¹⁰ not included unless they are the most abundant species.

^bAll of the metal is present in the vapor phase.

Table 5
Computed solubilities (in terms of mole fractions) of refractory metals in borosilicate glass melts at 1173 and 1273 K

Metal	T (K)	χ_m in melt
Re	1173	0.163
	1273	0.183
W	1173	0.0390
	1273	0.0570
Mo	1173	0.0809
	1273	0.113

glass where they can enhance ion emission probabilities by increasing the work function of the surface.

The present calculations were performed using the Facility for the Analysis of Chemical Thermodynamics (FACT) Gibbs free energy minimization code EQUILIB [35], which uses the chemical composition, pressure, temperature, an ensemble of possible phases, and thermodynamic quantities for those phases to deduce the state at which the free energy is at a minimum. Use of this code for this type of calculation has been previously described [4]. For the present work, it was necessary to merge data for additional chemical species into our user database. C_p 's for Re(g) and Re₂O₇(g) were taken from the HSC database of Roine and co-workers [36].

2.3. Chemical systems

Calculations were performed on model chemical systems consisting of B₂O₃, SiO₂, Re, and the analytes present as an oxide or nitrate. Each of the analytes considered has been reported to give the univalent atomic cation with the use of either borosilicate glass or with one of the other types listed in Table 1. The analyte elements (and their ionization potentials in eV) considered were lead (7.38), silver (7.45), thallium (6.07), tellurium (8.96), bismuth (7.29), cadmium (8.96), gold (9.18), iron (7.83), nickel (7.61), and chromium (6.74). Because of these high atomic ionization potentials (with the exception of Tl), the ion formation efficiency by a Saha-Langmuir process would be extremely low without some significant mechanism for increasing the work function of the surface. The chemical composition

considered was: 6.82×10^{-8} mol boron oxide, 2.00×10^{-8} mol silica, 9.27×10^{-9} mol of the analyte of interest, and 3.75×10^{-5} mol of Re filament material. This choice was based on three considerations. First, it was desired to choose molar amounts that were related to amounts of material used during the actual analyses. Second, the relative amounts of material (e.g. the relative amounts of the analyte, silica, and boron oxide) were chosen to be roughly equivalent to the ratios studied earlier [3,4]. Third, the amount of Re was chosen to correspond to a 0.001 in. \times 0.030 in. \times 0.67 in. Re filament; in addition, this amount of Re provides an essentially inexhaustible source of crystalline Re, consistent with the observation that the filament remains intact for the duration of the analysis.

The species and phases considered for the calculations were chosen as follows. For each calculation, every possible gaseous species was selected for consideration. This choice was made for two reasons. First, it was possible that an important species might be neglected if "chemical intuition" were used for gaseous species selection. Second, there was no need to limit the size of the ensemble of species and phases considered because the sizes of the chemical systems under consideration were well below the limitations of the code and the PC on which the calculations were performed. Re₂O₇ was the only Re–O vapor species considered although another Re oxide species, ReO₃, may also be present in the vapor phase over crystalline Re₂O₇ [37]. This choice was made because no thermodynamic data are available for ReO₃(g). In addition, the Re₂O₇(g) and Re(l) data had to be extrapolated outside their normal temperature ranges. The ramifications of the choices regarding the Re–O data are discussed later in more detail.

The liquid phase was considered as a single, ideal solution. The liquid species selected for consideration included: B₂O₃, SiO₂, Re, and phases involving the element of interest. As discussed previously, thermodynamic data for Re(l) were not available at the temperatures of interest, so the code was allowed to extrapolate the available data to this temperatures range.

The crystalline phases considered included (1) the

analyte of interest at the temperatures of interest, (2) any analyte metal borides, silicates and oxides for which there were data, and (3) the filament metal, filament metal oxides, borides, and silicates, etc. for which there were data. Because of the desire to address the reactivity of the melt with the other chemical species in the systems of interest, the crystalline phases SiO_2 and B_2O_3 were not considered for most calculations. Since glasses are by definition thermodynamically metastable, inclusion of these phases could deplete the glass of these species by precipitation of the crystalline phases, which is not consistent with the observed chemistry of these chemical systems.

3. Computational results

Calculations were performed for Pb, Tl, Te, Bi, Cd, Au, Fe, Ni, and Cr, as oxides, and Ag as AgNO_3 . The temperatures for the calculations were either (1) the temperatures at which published results have been reported for the analytes (as shown in Table 1) or (2) 1173 and 1273 K. The results of the calculations are presented in the ensuing sections; however, prior to presenting those results a few general comments about the results are presented. Also, in reviewing the data, it should be noted that for all ten elements some finite percentage of each analyte is reduced to the elemental state. This is an important result that supports the Saha-Langmuir model of ion formation.

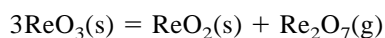
3.1. Thermodynamics of Re and Re–O phases

One of the hypothesized reasons for the success of the silica gel method is that Re and its oxides are solubilized by the glass phase, so it was imperative to include Re-bearing species and phases in the calculations. Re metal in the molten glass needs to be dealt with as a liquid, even though it is far below the melting temperature of pure Re, which leads to the need for extrapolating the liquid Re data to temperatures below the melting point.

It was likely that Re solubility was overestimated by this method. In an attempt to test this possibility,

an independent set of calculations was performed on other SiO_2 – B_2O_3 –M (M=metal) systems for which there were low temperature data for the metal. Mo and W were chosen because both are quite refractory, both have volatile oxides (as does Re), and there were complete data sets for the liquids at the temperatures of interest. Calculations for these systems at 1173 and 1273 K were compared to results for Re. These results are presented in Table 5. At 1173 K, Re solubility in borosilicate glass was predicted to be 2 and 4 times greater than the solubilities of Mo and W, respectively. At 1273 K, the Re solubility was predicted to be 1.5 and 3 times greater than the solubilities of Mo and W, respectively. If it is supposed that the chemistry of these three metals is similar, then it appears that the Re solubilities are overestimated by a factor of 2–4.

The only liquids in the Re–O system for which thermochemical data appear in the common thermodynamic databases are Re_2O_7 and Re, which is in agreement with the results of Battles et al. [37] and Skinner and Searcy [38]. These studies showed that both $\text{ReO}_2(\text{s})$ and $\text{ReO}_3(\text{s})$ disproportionate during high temperature vaporization by the following reactions:



There is a lack of data at higher temperatures for the crystalline Re–O phases. The CRC handbook [39] suggests that ReO_2 and ReO_3 decompose at 1273 and 673 K, respectively (without indicating the decomposition products). Greenwood and Earnshaw [40] give the decomposition temperature of 1173 K for ReO_2 by the previous reaction; Battles et al. [37] found that mixtures of ReO_2 and ReO_3 could be converted completely to ReO_2 by heating in vacuum at temperatures in the range 783–873 K. Although there are some inconsistencies associated with the decomposition temperatures of the ReO_2 and ReO_3 phases, it is concluded that the thermochemical data set for the condensed oxide phases of Re is adequate for this application.

The work of Battles et al. [37] and Skinner and

Searcy [38] suggest that there are most likely two vapor species, Re_2O_7 and Re , in equilibrium with ReO_2 and ReO_3 . These species were found to be quite abundant; however, it was not clear that the presence of a third, ReO_3 , was due to a process other than fragmentation of Re_2O_7 under electron bombardment. The uncertainty regarding the presence of $\text{ReO}_3(\text{g})$ over Re-O phases suggests that neglecting it in these calculations (if it is, in fact, an equilibrium species and not a fragmentation product) probably introduces little if any uncertainty to the results. It is possible, however, that glasses containing trace amounts of ReO_2 and/or ReO_3 could produce Re-O species other than those that are normally observed over the pure oxides.

3.2. PbO_2 , B_2O_3 , and SiO_2 with *Re filament*

Numerous measurements of the isotopic composition of Pb have been made by silica gel methods. The results reviewed during this computational study were primarily in the range 1373–1673 K [1,41–46], although one study was performed at 1773 K [42]. The equilibria of the borosilicate/molten glass system, with Pb present as PbO_2 , was considered at 100 K intervals in the range 1373 and 1673 K, which encompasses the range of temperatures from Table 1. $\text{Pb}(\text{g})$ is the most abundant Pb -bearing vapor species at all temperatures. At 1373 K the pressure is 8.84×10^{-9} atm; at 1673 K all of the Pb is in the vapor phase and the pressure is 9.19×10^{-9} atm. The most abundant Re -bearing species is Re_2O_7 . At 1373 K, the Re_2O_7 pressure is 2.22×10^{-9} atm; at 1673 K it is 4.16×10^{-16} atm (accompanied by increases in the partial pressures of O , O_2 , and Re). As the temperature is increased, the contribution of B-O species to the vapor phase increases, because of the volatility of B_2O_3 , until the glass phase is destroyed by vaporization of its components (between 1573 and 1673 K).

The calculations predict simple condensed phase chemistry. The only crystalline phase present at any temperature is Re . At 1373 K, the liquid solution includes 2.00×10^{-8} mol SiO_2 , 6.66×10^{-8} mol B_2O_3 , 2.51×10^{-8} mol Re , 1.51×10^{-13} mol Pb , and 6.70×10^{-15} mol PbO (the values for Pb and PbO are

not included in Table 6 because the minor species were truncated from the list of results). The mole fraction of B_2O_3 in the glass decreases with increasing temperature until the glass is destroyed by evaporation (between 1573 and 1673 K). The presence of Pb as $\text{Pb}(\text{II})$ is not unexpected. The work of Claussen and Russel [14] with high alkali content borosilicate glasses showed that $\text{Pb}(\text{II})$ was stable in the molten glass at temperatures up to 1373 K in air. This result is in contrast to the ion emitter work conducted under vacuum, which is a more reducing environment than air. To fully understand how the change in atmosphere impacts the oxidation states of the species in the glass will require additional experimental work.

3.3. AgNO_3 , B_2O_3 , and SiO_2 with *Re filament*

The silica gel results reported for experimental measurements for silver were obtained at 1273 K [44,47,48]; our calculations were performed at both 1173 and 1273 K. Most of these results were presented in an earlier publication [4], but are presented here along with newer results to allow comparison to those for the other analytes. This system shows essentially no reactivity other than the formation of a liquid solution of Re , Ag , B_2O_3 , and SiO_2 , and the reaction of Re with the oxygen supplied by the nitrate to form gaseous Re_2O_7 . At 1173 K, the liquid solution includes 2.00×10^{-8} mol SiO_2 , 6.82×10^{-8} mol B_2O_3 , 1.73×10^{-8} mol Re , 9.21×10^{-10} mol Ag . The vapor phase included only three species with pressures greater than 10^{-10} atm, Ag , N_2 and Re_2O_7 , with pressures of 8.35×10^{-9} , 4.64×10^{-9} , and 3.97×10^{-9} atm, respectively. The only crystalline phase predicted was Re . These calculations are not consistent with the experimental work, during which NO_2 was observed (as opposed to N_2). This suggests that at least some aspects of the decomposition process do not attain thermodynamic equilibrium. NO_2 is thermodynamically unstable, although it is commonly observed.

At 1273 K, the liquid solution includes 2.00×10^{-8} mol SiO_2 , 6.81×10^{-8} mol B_2O_3 , 2.11×10^{-8} mol Re , and 1.22×10^{-10} mol Ag . The vapor phase included only three significant species, Ag , N_2 , and

Table 6
Predicted speciation/phase behavior of metal oxides in glass, supported on Re

Initial phase	Temp (K)	Crystalline phases ^a	Glass speciation	Mole fraction ^b	Vapor speciation	Pressure (atm) ^c
PbO ₂	1573	Re	B ₂ O ₃	0.413	BO ₂	6.46 × 10 ⁻⁸
			SiO ₂	0.294	BO	1.83 × 10 ⁻⁸
			Re	0.293	Pb	9.22 × 10 ⁻⁹
					SiO	2.57 × 10 ⁻⁹
					B ₂ O ₃	2.28 × 10 ⁻¹⁰
AgNO ₃	1273	Re	B ₂ O ₃	0.623	Ag	9.15 × 10 ⁻⁹
			Re	0.193	N ₂	4.63 × 10 ⁻⁹
			SiO ₂	0.183	Re ₂ O ₇	3.94 × 10 ⁻⁹
			Ag	1.11 × 10 ⁻³	BO ₂	2.09 × 10 ⁻¹⁰
CdO	1573	Re	B ₂ O ₃	0.596	Cd	9.27 × 10 ⁻⁹
			SiO ₂	0.179	BO ₂	3.09 × 10 ⁻⁹
			Re	0.225	Re ₂ O ₇	1.02 × 10 ⁻⁹
Cr ₂ O ₃	1473	Re	B ₂ O ₃	0.553	BO ₂	1.52 × 10 ⁻⁹
			Re	0.242	BO	5.70 × 10 ⁻¹⁰
			SiO ₂	0.165	Cr	2.81 × 10 ⁻¹²
			Cr	2.02 × 10 ⁻⁵	CrO	1.11 × 10 ⁻¹²
			Cr ₂ O ₃	3.53 × 10 ⁻²	CrO ₂	5.05 × 10 ⁻¹³
			CrO	5.85 × 10 ⁻³		
FeO	1593	Re	B ₂ O ₃	0.329	BO ₂	7.30 × 10 ⁻⁸
			SiO ₂	0.353	BO	3.15 × 10 ⁻⁸
			Re	0.300	Fe	8.62 × 10 ⁻⁹
			FeO	9.85 × 10 ⁻³	SiO	7.62 × 10 ⁻⁹
			Fe	7.25 × 10 ⁻³	B ₂ O ₂	4.42 × 10 ⁻⁹
			Fe ₃ O ₄	2.58 × 10 ⁻⁸		
Fe ₂ O ₃	1593	Re	B ₂ O ₃	0.319	BO ₂	7.67 × 10 ⁻⁸
			Re	0.300	BO	2.90 × 10 ⁻⁸
			SiO ₂	0.362	Fe	8.55 × 10 ⁻⁹
			FeO	1.11 × 10 ⁻²	SiO	6.85 × 10 ⁻⁹
			Fe	7.19 × 10 ⁻³	B ₂ O ₂	3.76 × 10 ⁻⁹
NiO	1523	Re	B ₂ O ₃	0.493	BO ₂	2.56 × 10 ⁻⁸
			Re	0.276	BO	5.35 × 10 ⁻⁹
			SiO ₂	0.186	Ni	4.52 × 10 ⁻⁹
			Ni	4.46 × 10 ⁻²	B ₂ O ₂	5.98 × 10 ⁻¹⁰
			NiO	2.62 × 10 ⁻⁴	SiO	3.42 × 10 ⁻¹⁰
TeO ₂	1573	Re	B ₂ O ₃	0.413	BO ₂	6.46 × 10 ⁻⁸
			Re	0.293	BO	1.83 × 10 ⁻⁸
			SiO ₂	0.294	Te	9.26 × 10 ⁻⁹
					SiO	2.57 × 10 ⁻⁹
					B ₂ O ₂	2.28 × 10 ⁻⁹
Tl ₂ O ₃	973	Re	B ₂ O ₃	0.689	Tl	1.85 × 10 ⁻⁸
			Re	0.108	Re ₂ O ₇	3.97 × 10 ⁻⁹
			SiO ₂	0.202		
			Tl	1.79 × 10 ⁻⁴		
Bi ₂ O ₃	1273	Re	B ₂ O ₃	0.624	Bi	9.27 × 10 ⁻⁹
			Re	0.193	Re ₂ O ₇	1.96 × 10 ⁻⁹
			SiO ₂	0.183	BO ₂	1.99 × 10 ⁻¹⁰

(continued on next page)

Table 6 (continued)

Initial phase	Temp (K)	Crystalline phases ^a	Glass speciation	Mole fraction ^b	Vapor speciation	Pressure (atm) ^c
Au ₂ O ₃	1273	Re	B ₂ O ₃	0.566	Re ₂ O ₇	1.96 × 10 ⁻⁹
			Re	0.193	Au	3.38 × 10 ⁻¹⁰
			SiO ₂	0.166	BO ₂	1.90 × 10 ⁻⁹
			Au	7.43 × 10 ⁻²		

^aListed in order of descending quantities.

^bValues less than 10⁻⁵ not listed.

^cValues less than 10⁻¹⁰ not included unless they are the only species for the metal of interest.

Re₂O₇, with pressures of 9.15 × 10⁻⁹, 4.63 × 10⁻⁹, and 3.93 × 10⁻⁹ atm, respectively. At this temperature, the only crystalline phase predicted was Re.

An additional set of calculations that included AgNO₃(l) as one of the possible liquid species was performed at 1173 and 1273 K, even though AgNO₃ is believed to decompose at temperatures in the range 583–873 K, [39,49,50] to see if the amount of Ag(I) present in the melt could be determined. The results of these calculations predicted a very small amount of Ag⁺ would be present in the melt, with mole fractions of 7.8 × 10⁻³³ and 2.0 × 10⁻³² at 1173 and 1273 K, respectively. This computed result is in contrast to the work of others who have detected abundant Ag⁺ in molten alkali containing silicate [22], borosilicate [34], and aluminosilicate [19] melts by cyclic voltammetry. It is suspected that this somewhat poor agreement is due to the kinetics of the reactions in these viscous molten glass systems, and the different conditions associated with the mass spectrometer experiments (under high vacuum conditions) and the electrochemistry experiments (exposed to an oxidizing atmosphere).

3.4. CdO, B₂O₃, and SiO₂ with Re filament

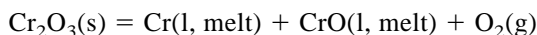
Calculations for this chemical system were performed in the interval 1373–1673 K [41,44,51,52]. Cadmium was predicted to be almost entirely partitioned to the vapor phase. The computed Cd pressures were essentially constant over the 400 K range, near 9.3 × 10⁻⁹ atm, because CdO is expected to completely decompose under these conditions to produce Cd(g) and O(g) or O₂(g), with the amount of Cd

present in glass governed by the equilibria between Cd(g) and the glass phase. As the temperature increases over the range studied, the glass phase becomes increasingly B₂O₃ depleted until it decomposes, releasing B, Si, O, and Cd to the vapor phase. The vapor pressure of Re at each temperature is very low (in the 10⁻¹⁹ to 10⁻²¹ atm range). Because of its low vapor pressure, Re is expected to contribute little to the vapor phase other than through the formation of Re₂O₇, which is probably the major pathway to depletion of Re from the filament. The only crystalline phase predicted is Re; over 99% of the Re is expected to be present as unreacted, crystalline Re.

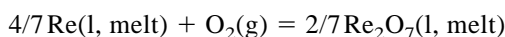
3.5. Cr₂O₃, B₂O₃, and SiO₂ with Re filament

This chemical system was analyzed over the 1423–1523 K range, which encompasses the ranges of temperatures for which experimental results have been published [53,54]. As the temperature was increased, the calculations predicted depletion of B₂O₃ and SiO₂, with more depletion of B₂O₃ due to its greater volatility. As the temperature increased, the amount of Cr in the glass increased, while the amounts of CrO and Cr₂O₃ in the glass decreased with increasing temperature. The amounts of Re in the glass, vapor and crystalline phases were essentially unchanged over this 100 K range, with over 99% of the Re present as Re(s). The most abundant Cr-bearing vapor species predicted were Cr and CrO. The pressures of these species increased with the temperature, from 2.81 × 10⁻¹² and 1.11 × 10⁻¹² atm at 1423 K to 7.52 × 10⁻¹¹ and 2.67 × 10⁻¹¹ atm at 1523 K.

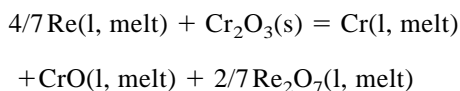
At these temperatures, it appears that dissolution of Cr_2O_3 to form Cr and CrO in the glass proceeds by a two-step process, with small amounts of Re_2O_7 generated from the reaction of Re with oxygen released during the Cr_2O_3 dissolution, Reaction A:



Reaction B:



as opposed to Re reducing Cr_2O_3 in a single step to form Cr, CrO and Re_2O_7 , Reaction C:



This assertion that the dissolution of Cr_2O_3 in the molten glass is necessary for the subsequent formation of Re_2O_7 is based on an additional set of calculations, performed on a chemical system with Re and Cr_2O_3 , that showed Re does not reduce crystalline Cr_2O_3 at these temperatures. The prediction that Cr(III) is present in the glass phase appears to be reasonable, based on the results of Medlin and co-workers [25] and Russel and von der Gonna [28], who were both able to detect Cr^{3+} in silicate-based glass melts.

3.6. $\text{Fe}_2\text{O}_3/\text{FeO}$, B_2O_3 , and SiO_2 with Re filament

Two sets of calculations were performed: in the first, Fe was introduced as Fe_2O_3 ; in the second as FeO. The temperatures at which the calculations were performed were 1423, 1593, and 1613 K, which includes the temperatures at which experimental results have been published [2,55,56]. The two sets of calculations gave very similar results. For both chemical systems, and at all temperatures considered, the predicted crystalline phases were essentially identical. Re was the only solid present, and in all cases over 99% of the Re was crystalline. The glass composition showed variations related to temperature changes and chemical composition changes. In general, as the temperature was increased from 1423 to 1613 K the

glass phase was preferentially depleted of B_2O_3 , with a considerably lesser depletion of SiO_2 , and the solubilities of the solutes, Re, Fe, FeO, and Fe_3O_4 were reduced as the temperature increased. As expected, the FeO calculations result in the greatest pressure of Fe in the vapor phase and the Fe_2O_3 calculations resulted in higher pressures of FeO. The predicted Re_2O_7 pressures were about two times greater in the Fe_2O_3 calculations, which is not surprising since this system contains additional oxygen.

Additional calculations showed that Re does not reduce FeO or Fe_2O_3 under these conditions. Instead, it is the dissolution of the Fe–O phases by the glass phase that liberates oxygen that is present in Re_2O_7 . The presence of Fe(III) is in agreement with the results of others [12,13,25] who all detected it in borosilicate glass melts. In addition, Medlin and co-workers [25] also detected Fe(II).

3.7. NiO , B_2O_3 , and SiO_2 with Re filament

Experimental work on this system has been performed at 1523 K [53,57]. Because of the high temperature, calculations predict that the glass phase is preferentially depleted of B_2O_3 , which is lost to the vapor phase. Ni is the most abundant Ni-bearing species in the vapor phase, whereas NiO is the most abundant Ni-bearing component in the glass phase. Re is the only crystalline phase predicted at this temperature. The small amount of Re not present in the crystalline or glass phase is present as vapor species formed at the expense of the NiO. The prediction that Ni(II) would be present in the melt is not surprising, as Medlin and co-workers [25] detected Ni(II) in borosilicate glass melts.

3.8. TeO_2 , B_2O_3 , and SiO_2 with Re filament

Published silica gel results for Te are at a high experimental temperature, 1523 K, [47,58] which is above the normal boiling point of both Te and TeO_2 . The higher than expected experimental temperature (as compared to the computational results) is probably related to the chemistry of the borosilicate glass solution formed with TeO_2 .

The modeling results predicted that Re was the only crystalline phase at this temperature. Over 30% of the B_2O_3 is lost to the vapor phase by the time the system reaches equilibrium. The mole fraction of Te in the melt is quite small, $\chi = 10^{-7}$, with the remainder of the Te present in the vapor phase, primarily as Te at a pressure of 9.25×10^{-9} atm. The behavior of Te and Re in this system is what would be expected. TeO_2 boils at about 1518 K [39], so it is not surprising that little TeO_2 is present in the melt ($\chi = 10^{-14}$). The presence of Te(IV) is in agreement with the results of Claussen and Russel [14] who detected Te^{4+} and Te^{6+} in alkali-containing borosilicate glass melts at 1273 K. It is possible that the solution is more stable, with regard to the ability of Te to escape, than the ideal solution upon which the modeling results are based.

3.9. Tl_2O_3 , B_2O_3 , and SiO_2 with Re filament

The only published temperature for the silica gel method involving Tl was 973 K [41,59]. This temperature is below the melting point of Tl_2O_3 , 1107 K. The only crystalline phase predicted is Re(s), where over 99% of the Re resides. Over 99% of the Tl is predicted to be present in the vapor phase, entirely as Tl, with a vapor pressure of 1.85×10^{-8} atm. The destruction of Tl_2O_3 is due to the ability of Re(s) to react with it to form $Re_2O_7(g)$.

3.10. Bi_2O_3 , B_2O_3 , and SiO_2 with Re filament

In the temperature range 1173–1273 K, both Bi and Bi_2O_3 are liquids, so it was expected that Bi would be present only in the liquid and vapor phases; the computed results were in agreement with this expected behavior. Essentially all of the Bi_2O_3 present in the melt is reduced by Re to Bi^0 . The mole fraction of Bi_2O_3 in the glass was in the 10^{-14} – 10^{-15} range at these temperatures, whereas the mole fraction of Bi in the glass was considerably larger, approximately 0.005. Re was predicted to be present in the solid, liquid and vapor phases at both temperatures. The only crystalline phase predicted was Re. The predicted pressures of Re_2O_7 were 1.98×10^{-9} atm at

1173 K and 1.96×10^{-9} atm at 1273 K. At both temperatures Bi(g) was the most abundant Bi-bearing species, at a pressure of 9.27×10^{-9} atm at both temperatures. The presence of Bi(III) in the melt is in agreement with the results of Claussen and Russel, [13] who detected Bi(III) in borosilicate glass melts.

3.11. Au_2O_3 , B_2O_3 , and SiO_2 with Re filament

In the temperature range 1173–1273 K, the computed results for this chemical system are quite similar to the Bi_2O_3 -containing system; however, the high temperature chemistry of the Au–O system is more like the Ag–O system than the Bi–O system. Au_2O_3 decomposes at about 500 K. At the high temperatures of this study, oxygen has essentially no solubility in gold. The calculations predict that essentially all of the Au present in the melt, 9.25×10^{-9} mol, is present as Au. It is predicted that Re will react with the oxygen liberated by $Au_2O_3(s)$ to form $Re_2O_7(g)$, 1.98×10^{-9} atm at 1173 K and 1.96×10^{-9} atm at 1273 K. Au(g) was the only gold-bearing vapor species considered in these calculations, and was predicted to be present at pressures of 2.17×10^{-11} atm at 1173 K and 3.38×10^{-10} atm at 1273 K.

4. Discussion

The differences between the experimental and calculated temperatures at which 50% of the solute metals would be expected to evaporate from the molten glass indicates that kinetic factors, perhaps related to processes that are not understood, are significant contributors to the chemistry of these systems. Nevertheless, there are a number of characteristics elucidated by these calculations that provide new insights into possible ion emission mechanisms that may help to explain at least some of the unresolved issues associated with the chemistry of the silica gel method.

One significant issue is that, other than for Ag, these elements do not exhibit a stable univalent cation in the condensed phase, while the univalent cation appears to be the only ion emitted from the molten

glass matrix. The results of the voltammetry experiments on borosilicate glass melts to identify the oxidation states of dissolved elements showed that, other than for Ag, none of the elements of interest that were studied by voltammetry in molten glass (Cr, Ni, Te, Pb, Bi, and Fe) were present as other than multiply charged or neutral species. The formation of a singly charged gas phase ion directly from a multiply charged ion dissolved in molten glass is unlikely, suggesting that singly charge species originate as neutral species in the melt that are stripped of an electron during volatilization. The computational results are consistent with this model.

One common result for all of the calculations is the prediction that a finite amount of each analyte is present in the elemental state in both the molten glass and the vapor phase. These “solubilization” and “reduction” phenomena in the molten borosilicate glass may be important features of the process, since they suggest that the analyte atoms are, for the most part, independent of one another and that these atoms evaporate, at least in part, as single atoms (either as a neutral or singly charged ionic species). The significance of the solubilization of the reduced analyte atoms is that this phenomena supports the notion that the neutral monatomic elemental vapor species and monatomic, singly charged thermal ions could be produced from the same species in the molten glass, namely, the analyte in the elemental state. If this is the case, it is possible that these ion formation processes are a Saha-Langmuir type process. This issue will be addressed in more detail later.

4.1. Reconciliation of the experimentally observed and computational results

If the evaporation coefficients are close to unity, the computed equilibrium vapor pressures probably correspond to the lower limit for the glass evaporation rate. In a “free evaporation” process such as this the condensed and vapor phases are not in equilibrium. Because the vacuum pumps and cool walls of the mass spectrometer are removing the vapor phase, there is continual loss of material (as in the transpiration process) until the condensed phase is ex-

hausted. However, it is likely that these calculations overestimate the evaporation loss due to the fact that the estimated temperatures for loss of ~50% of the analyte in a 40 min time period are well below the experimental temperatures of the analyses for most of these elements. Quite possibly this is due to the high viscosities of the molten glasses. Since sample is almost always left at the end of an analysis, even though the experimental temperatures are considerably above those predicted by the calculations, the evaporation coefficients must be far less than unity.

The computational results in Table 6 show the vaporization of the oxides or nitrates of Pb, Ag, Cd, Cr, Fe, Ni, Te, Tl, Bi, and Au from a borosilicate glass matrix. The calculations predict a vapor phase with the most abundant of the species of the element of interest in the zero oxidation state. In these systems, the elemental oxide (or nitrate), initially present as a solid, is reduced. This reduction is due to one of two phenomena. Either (1) the condensed-phase oxide or the oxide vapor species are thermodynamically unstable with regard to decomposition to the elemental species at the temperature of interest (either due to the decomposition of the oxide or due to the preferential solubility of the metal in the glass phase), or (2) Re reduces the oxide, resulting in $\text{Re}_2\text{O}_7(\text{g})$ and the element. The predicted high temperature chemical equilibria of various pure metal oxides are presented in Table 4. As can be seen in Table 4, the first phenomenon is clearly important for Ag, Cd, Cr, Fe (as FeO and Fe_2O_3), Ni, Tl, Bi, and Au.

Calculations were performed to compare the vapor pressures of the elements in borosilicate glass to those of the pure elements. These results (presented in Table 3) were used to test the hypothesis that emission of thermal ions from molten glass ion emitters is enhanced because the analysis temperature is significantly increased. The reference temperature of 1173 K was chosen for these calculations because it was the lower limit of the temperature range involving studies of the bismuth-silica gel [3] and silver-silica gel systems [4]. As would be expected, the vapor pressures predicted from the glass solution calculations were lower than those predicted for the pure elements. This is because the fugacities of these elements in the

glass solution are less than their fugacities in the pure materials; however, this difference is quite small and cannot explain a significant enhancement in ion emission. The chemistry of these systems is more likely to be dominated by the kinetics of the analyte species migrating through the highly viscous molten glass.

Neutral, monatomic analyte species were predicted (by the thermochemical calculations) to be present in both the molten glass and the vapor phase for all of the analytes considered. Therefore, it is suspected that the formation of ions detected over these molten glasses (experimentally) may be related to a Saha-Langmuir type process. In an attempt to test this possibility, the observed emission of thermal ions and the computed equilibrium vapor pressures were compared. For situations in which vapor species impinge on a surface and are re-emitted as either an ionic or a neutral species, the ion to neutral emission ratio for a specific material may be predicted using the Saha-Langmuir equation

$$\frac{n_+}{n_0} = \frac{g_+}{g_0} \frac{(1 - r_+)}{1 - r_0} \exp \frac{(\phi - \text{IP})}{RT}$$

(in which ϕ is the work function of a surface at which ionization is occurring, IP is the ionization potential of the ions formed, g_+ and g_0 are the respective statistical weights for the ion and its related neutral vapor species, r_+ and r_0 are the respective reflection coefficients for the ion and neutral species, R is the gas constant, T is the absolute temperature, and n_+/n_0 is the emission ratio of positive ions to neutral species leaving the surface).

Although it is not expected that the Saha-Langmuir theory should be an exact fit when applied to these conditions (which are different than those assumed during the development of the mathematical expression), the theory might be used to explain trends in the behavior of these chemical systems. For materials in which the work function of the condensed phase is less than the first ionization potential for gaseous species, raising the temperature increases the positive ion to neutral ratio. The ionization potential of each of these metals, except Tl and Cr, is more than 7eV. Using the Saha-Langmuir equation, a work function

of 5eV, and an ionization potential of 7 eV, at $T = 1000$ K an ion ratio of about 10^{-10} is obtained. Since the pressures of the neutral species at these temperatures are less than 10^{-7} atm, this result predicts that the ion pressures are about 10^{-17} to 10^{-20} atm, which would result in an ion beam of too low an intensity to be detected. These results suggest that either another phenomenon (other than a Saha-Langmuir type process) contributes to the formation of ions in the silica gel method, or that the work function of the surface is much higher than would be surmised from existing measurements of the work function on similar surfaces.

It appears that a number of factors impact ion emission from these molten glasses. Past work on the silver- [4] and bismuth-borosilicate systems [3] brought to light what were hypothesized to be two important roles the molten glass plays in the ionization process. First, it acts as a solvent for the analytes and Re and second, it provides the oxygen necessary to oxidize the Re present in the glass. In most of the calculations, the most abundant vapor species predicted were those related to the evaporation of the glass matrix itself. B_2O_3 is particularly volatile (as compared to SiO_2), forming $\text{BO}_2(\text{g})$ and $\text{BO}(\text{g})$, although the comparison of the calculated and experimental temperatures suggests that the vaporization coefficients are quite low, and that the calculations probably provide an upper limit to the extent of this type of glass phase decomposition. Re_2O_7 is also an important vapor species, especially in those systems in which Re readily reduces the analyte. It is hypothesized that the presence of $\text{Re}_2\text{O}_7(\text{g})$ (predicted by the thermochemical modeling) and $\text{ReO}_4^-(\text{g})$ (observed during studies of the bismuth borosilicate system [3]) are indicative of the significant role the presence of Re plays in the thermal ion emission process.

4.2. Comparison of computed and experimental temperatures

When comparing the temperatures at which silica gel samples were analyzed (Table 1) to the computed temperatures at which approximately 50% of the sample would be depleted in 40 min (Table 2), it was found that the latter temperatures were in all cases,

except for Cr, lower than the experimental temperature at which the analysis was run. For the oxides NiO, FeO, and Cr₂O₃, the temperatures are in reasonable agreement (less than 200 K difference between the two temperatures). For PbO₂, AgNO₃, CdO, and Te₂O₃ the calculated temperatures are 300–900 K lower than the experimental temperatures. Understanding the cause of these divergent behaviors could lead to a better understanding of the actual chemical and physical processes that control the ion emission process of the silica gel method.

Although the observed discrepancies between the experimental and calculated results is thought to be, in part, an artifact due to the assumption that the molten glass solution was ideal and kinetic factors were ignored, it is likely that other factors are important. Retarded vaporization (characterized by a vaporization coefficient less than unity) could lead to the observed discrepancy between the computational results and the experimental results. The causes of retarded vaporization are not well understood; however, it is supposed that surface effects (homogeneity and purity) and possible localized deviations in the surface temperature are related to the phenomenon, as well as the kinetics of the analyte diffusing through the molten glass. The observed deviations of the evaporation rates (computed rates being greater than experimentally observed rates) in the chemical systems under consideration support the argument that retarded vaporization plays a role in the chemical behavior of these systems. This behavior is not uncommon and is exhibited by other B₂O₃-containing systems, such as the B₂O₃-GeO₂ system, for which the vaporization coefficients of GeO are near 0.03 over a wide composition range of compositions, $\chi_{\text{GeO}} = 0.1\text{--}0.5$ [60].

Another significant observation is that the computed and experimental results for elements analyzed at the higher temperatures (Cr, Ni, and Fe) are in closer agreement than those analyzed at the lowest temperatures (Ag, Pb, Bi, Te, Tl, and Cd). This behavior could be related to the viscosity of the glass; at higher temperatures the glass is less viscous and the diffusion rates of solute species would be expected to increase with the decrease in viscosity. Based on the

experimental and modeling results, it appears that the temperature of the melt must be above about 1200 K before appreciable migration can occur, regardless of the calculated vapor pressure of the species being analyzed.

A comparison of Tables 4 and 6 shows that the thermodynamic calculations predict a substantial change in the chemistry of these elemental oxides and nitrates in going from the pure state to being dissolved in molten glass at comparable elevated temperatures. In particular, there is a shift toward a higher percentage of the element in the zero oxidation state in the gas phase. In the case of silver, which has been studied both experimentally and computationally, the thermodynamics are such that this chemical reduction is independent of the presence of the glass phase. For other elements that are more difficult to reduce, it appears that the molten glass matrix has a significant role in the reduction to the elemental state. An important aspect of these chemical systems is that the analyte element resides in the molten glass in the elemental state and can volatilize as individual atoms.

Last, a significant enhancement in the work function of the surface of the molten glass is required to explain the experimentally observed ion formation efficiencies. A work function of at least 6 eV or higher is required to explain these efficiencies. A presence of Re oxides on the surface of the molten glass can explain this enhancement; Davis made measurements showing that the work function of an oxidized Re surface can be as high as 7.2 eV [61].

5. Conclusions

Although additional experimental work will be required to definitively characterize the silica gel process, there are some insights that may be gleaned from the present and past work in this area. Of particular significance are our past results [3,4] and those of Davis [61], Medlin and co-workers [25], and Claussen and Russel [12–14]. Our previous work showed that ions originate at the surface of the borosilicate glass. This result is significant because it precludes ion formation by an alternative means that

involves ionization at the Re filament, such as evaporation of neutrals from the glass that subsequently encounter the Re filament and are ionized (as in the case with the double- or triple-filament thermal ion source). The work of Davis indicates that the work function of oxidized Re surfaces is much greater than that of Re, which suggests that the work function of molten borosilicate glass could be modified by the Re–O species that are at the surface during volatilization. This interpretation is in agreement with our past results [3] which showed that $\text{ReO}_4^-(\text{g})$ was emitted from the same location on the glass surface as the $\text{Bi}^+(\text{g})$ thermal ions. In addition, the present computational results predict that considerable Re is dissolved in the molten glass ion emitter and that $\text{Re}_2\text{O}_7(\text{g})$ is expected to be present over the glass phase at high temperatures.

The results of Medlin and co-workers, and Clausen and Russel, demonstrate that singly charged species (for a variety of transition and main group elements other than Ag) are not present in borosilicate glass melts. This means that the ion formation process for singly charged ions must be a surface phenomena that is most likely governed by the work function at the melt–vapor interface, as opposed to the simple vaporization of ionic species already present in the glass melt.

This model for ion formation from the molten glass ion emitters is based on the belief that the univalent thermal ions measured in the mass spectrometer originate in the melt as neutral, monatomic species that migrate to the surface where they form ions with adequate thermal energy to vaporize. Neutral and oxidized (non-univalent species for all analytes other than Ag) species of each analyte are solvated in the molten glass. As neutral species migrate to the surface they volatilize with some fraction stripped of an electron to form a positive ion as they leave the surface. The ratio of ions to neutrals is determined by the difference in the values of the work function of the surface and the ionization potential of the evaporating species. Dissolved Re (from the filament) is oxidized to form the ReO_x (an Re–O species or phase of unknown composition) required to increase the work function of the glass, thus enhancing the formation of

thermal ions from the surface of the molten glass. The decrease in concentration of neutral analyte atoms causes a shift in the ion-neutral equilibria in the melt, causing more neutral species to be formed, allowing a higher percentage of the analyte to be converted to gas phase ions by way of the above-mentioned process.

Ag and Au appear to be the elements that best fit the proposed model, since no oxide or nitrate of Ag or Au appears to be stable at temperatures approaching those used for analysis, whether in the pure form or in the borosilicate matrix. In addition, the calculations predict that a reasonable percentage of the other eight elements could also reside in the elemental state in both the borosilicate glass and gas phases.

Last, emission of pre-formed ions is not supported by the data. None of these elements other than Ag has a stable univalent cationic state, and Ag appears to be present predominantly in the elemental state. Multiply charged ions for most elements are probably present to some extent in the molten glass, but would not be expected to be observed in the mass spectrometer due to the energetics required for them to be released into the gas phase. Thus, it is likely that all ten of these elements, when ionized by the silica gel method, are first reduced to the elemental state and then stripped of an electron during volatilization by a Saha-Langmuir type ion formation process.

Acknowledgments

This work was supported by the U.S. Department of Energy, Office of Science, Basic Energy Sciences, under program no. 3ED102.

References

- [1] A.E. Cameron, D.H. Smith, R.L. Walker, *Anal. Chem.* 41 (1969) 525.
- [2] A. Götz, K.G. Heumann, *Int. J. Mass Spectrom. Ion Processes* 83 (1988) 319.
- [3] T. Huett, J.C. Ingram, J.E. Delmore, *Int. J. Mass Spectrom. Ion Processes* 146/147 (1995) 5.
- [4] G.F. Kessinger, T. Huett, J.E. Delmore, *Int. J. Mass Spectrom.*, in press.
- [5] V.S. Fomenko, *Handbook of Thermionic Properties*, Elec-

- tronic Work Functions and Richardson Constants of Elements and Compounds, Plenum, New York, 1966, p. 69.
- [6] P. Buhler, *Glass Phys. Chem.* 24 (1998) 515.
- [7] P. Buhler, *Glass Phys. Chem.* 24 (1998) 521.
- [8] P. Buhler, *Glass Phys. Chem.* 24 (1998) 387.
- [9] P. Buhler, *Glass Phys. Chem.* 24 (1998) 392.
- [10] P. Buhler, *Glass Phys. Chem.* 25 (1999) 172.
- [11] O. Claussen, C. Russel, *Glastechnische Berichte-Glass Sci. Technol.* 69 (1996) 95.
- [12] O. Claussen, C. Russel, *Berichte Der Bunsen-Gesellschaft-Phys. Chem. Chem. Phys.* 100 (1996) 1475.
- [13] O. Claussen, C. Russel, *Phys. Chem. Glass.* 38 (1997) 227.
- [14] O. Claussen, C. Russel, *J. Non-Cryst. Solids* 209 (1997) 292.
- [15] O. Claussen, C. Russel, *Glastechnische Berichte-Glass Sci. Technol.* 70 (1997) 231.
- [16] O. Claussen, C. Russel, *J. Non-Cryst. Solid* 215 (1997) 68.
- [17] O. Claussen, C. Russel, *Phys. Chem. Glass.* 39 (1998) 200.
- [18] O. Claussen, C. Russel, *Solid State Ion.* 105 (1998) 289.
- [19] O. Claussen, C. Russel, *J. Mol. Liq.* 83 (1999) 295.
- [20] O. Claussen, S. Gerlach, C. Russel, *J. Non-Cryst. Solids* 253 (1999) 76.
- [21] S. Gerlach, O. Claussen, C. Russel, *J. Non-Cryst. Solids* 248 (1999) 92.
- [22] M. Maric, M. P. Brungs, M. Skyllaskazacos, *Phys. Chem. Glass.* 30 (1989) 12.
- [23] A. Matthai, O. Claussen, D. Ehrh, C. Russel, *Glastechnische Berichte-Glass Sci. Technol.* 71 (1998) 29.
- [24] A. Matthai, D. Ehrh, C. Russel, *Glass Sci. Technol.-Glastechnische Berichte* 73 (2000) 33.
- [25] M.W. Medlin, K.D. Sienert, H.D. Schreiber, *J. Non-Cryst. Solids* 240 (1998) 193.
- [26] C. Russel, *Phys. Chem. Glass.* 32 (1991) 138.
- [27] C. Russel, S. Gerlach, *Ceram.-Silikaty* 43 (1999) 165.
- [28] C. Russel, G. von der Gonna, *J. Non-Cryst. Solids* 260 (1999) 147.
- [29] N. Takeshima, M. Koide, K. Matusita, *J. Ceram. Soc. Jpn.* 107 (1999) 875.
- [30] N. Takeshima, M. Koide, K. Matusita, *J. Ceram. Soc. Jpn.* 108 (2000) 504.
- [31] G. von der Gonna, C. Russel, *Glass Sci. Technol.-Glastechnische Berichte* 73 (2000) 105.
- [32] G. von der Gonna, C. Russel, *J. Non-Cryst. Solids* 262 (2000) 236.
- [33] H. Yamashita, S. Yamaguchi, M. Yokozeki, M. Nakashima, T. Maekawa, *J. Ceram. Soc. Jpn.* 107 (1999) 895.
- [34] K. Yata, N. Hanyu, T. Yamaguchi, *J. Am. Ceram. Soc.* 78 (1995) 1153.
- [35] C.W. Bale, A.D. Pelton, W.T. Thompson, *Facility for the Analysis of Chemical Thermodynamics (F*A*C*T) 2.1-User Manual*, Ecole Polytechnique de Montreal, Montreal, Quebec, Canada/Royal Military College, Kingston, Ontario, Canada, 1996.
- [36] A. Roine, *HSC Chemistry for Windows 3.0'*, Outokumpu Research Oy, Pori, Finland, 1997.
- [37] J.E. Battles, G.E. Gunderson, R.K. Edwards, *J. Phys. Chem.* 72 (1968) 3963.
- [38] H.B. Skinner, A.W. Searcy, *J. Phys. Chem.* 77 (1973) 1578.
- [39] *CRC Handbook of Chemistry and Physics*, R.C. Weast (Ed.), CRC Press, Boca Raton, FL, 1983, p. B-130.
- [40] N.N. Greenwood, A. Earnshaw, *Chemistry of the Elements*, Pergamon, Elmsford, NY, 1984, p. 1218.
- [41] E. Waidmann, K. Hilpert, J.D. Schlodot, M. Stoeppler, *Fres. Z. Anal. Chem.* 317 (1984) 273.
- [42] F. Tera, G. J. Wasserburg, *Anal. Chem.* 47 (1975) 2214.
- [43] J.D. Schlodot, K. Hilpert, H.W. Nürnberg, *Adv. Mass Spectrom.* 8A (1980) 325.
- [44] K.J.R. Rosman, J.R. De Laeter, A. Chegwidden, *Talanta* 29 (1982) 279.
- [45] B.V. L'vov, A.V. Novichikhin, *Spectrochim. Acta Part B* 50 (1995) 1427.
- [46] I.L. Barnes, T.J. Murphy, J.W. Gramlich, W.R. Shields, *Anal. Chem.* 45 (1973) 1881.
- [47] R.D. Loss, K.J.R. Rosman, J.R. De Laeter, *Talanta* 30 (1983) 831.
- [48] W.R. Kelly, F. Tera, G.J. Wasserburg, *Anal. Chem.* 50 (1978) 1279.
- [49] M. Afzal, M. Saleem, H. Ahmad, *Sci. Int. (Lahore)* 2 (1990) 285.
- [50] D.J. Anderton, F.R. Sale, *Proceedings of the First European Symposium on Thermal Analysis*, University of Salford, UK, 1976, p. 278.
- [51] A. Broekman, J.G. van Raaphorst, *Fres. Z. Anal. Chem.* 318 (1984) 398.
- [52] K.J.R. Rosman, J.R. De Laeter, *Int. J. Mass Spectrom. Ion Phys.* 16 (1975) 385.
- [53] J.L. Birck, G.W. Lugmair, *Earth Planet. Sci. Lett.* 90 (1988) 131.
- [54] G.W. Lugmair, A. Shukolyukov, *Geochim. Cosmochim. Acta* 62 (1998) 2863.
- [55] P.R. Dixon, R.E. Perrin, D.J. Rokop, R. Maeck, D.R. Janecky, J.P. Banar, *Anal. Chem.* 65 (1993) 2125.
- [56] P.D.P. Taylor, R. Maeck, P. De Bièvre, *Int. J. Mass Spectrom. Ion Process.* 121 (1992) 111.
- [57] A. Shukolyukov, G. W. Lugmair, *Science* 259 (1993) 1138.
- [58] C.L. Smith, J.R. De Laeter, K.J.R. Rosman, *Geochim. Cosmochim. Acta* 41 (1977) 676.
- [59] E. Waidmann, K. Hilpert, M. Stoeppler, *Fres. J. Anal. Chem.* 338 (1990) 572.
- [60] V. L. Stolyarova, G. A. Semenov, *Mass Spectrometric Study of the Vaporization of Oxide Systems*, Wiley, New York, 1994, p. 33.
- [61] W.D. Davis, *Environ. Sci. Technol.* 11 (1977) 587.